Practical Considerations for Estimating Road Vehicle Frequency Response Functions from Response Data

Practical considerations for estimating road vehicle frequency response functions from response data

Daniel Ainalis[1*], Vincent Rouillard[1] and Michael Sek[1]

[1] *College of Engineering and Science, Victoria University, Australia*

[*] *Corresponding author. Email: Daniel.Ainalis@vu.edu.au*

Abstract: This paper describes the application of a practical method to estimate the dynamic characteristics (frequency response function) of road vehicles using only on-the-road vertical vibration response data measured during nominally constant operating speeds. While several methods exist to estimate these dynamic characteristics, they are generally either inexact or prohibitively resource intensive. A review of two analytical approaches for estimating the frequency response function of road vehicles using only on-the-road vibration response data is presented. The first approach is based on the assumption that the road elevation profile takes the form of a specified spectral function. The second approach is based on the random decrement technique. A practical, step-by-step guide to undertaking on-the-road vehicle vibration measurements is included and provides numerous useful tips and considerations that should be taken into account. An investigation was also undertaken into the minimum record length (i.e. fraction of road length) required to accurately estimate the dynamic characteristics of road vehicles using a Monte Carlo simulation. From the study, it was found that a minimum road length of 10 – 15 km is sufficient to obtain a reasonably accurate estimate.

Keywords: Road vehicle vibration, frequency response function, random decrement, vibration record length, Monte Carlo simulation

1.0 Introduction

As the volume of products transported by road continues to rapidly increase it is becoming ever more important to use an optimal level of protective packaging to safeguard products from road vehicle vibration during transportation. The significant costs associated with inadequate or excess packaging further reinforce the need to develop improved approaches for the testing and optimisation of product-packaging systems to prevent damage during transportation [1]. Evaluating various protective packaging systems through actual trial shipments is impractical and expensive, leading to testing in the laboratory as an increasingly valid and widely implemented alternative [2]. This paper presents an overview of a state-of-the-art method for simulating realistic transportation vibration. Next, a review of two recently developed techniques to estimate the dynamic characteristics, namely the Frequency Response Function (FRF), of road vehicles using only on-the-road vibration response data is given. The results of a Monte Carlo simulation are then presented, which aimed to provide an initial investigation into the minimum length of road required to undertake these on-the-road measurements. Finally, a section discussing the various considerations which have to be made to undertake the experimental measurements is presented.

2.0 Simulating Realistic Vehicle Distribution Vibrations

The simulation of realistic vehicle vibrations for testing and characterisation is useful for many applications, notably in the design and optimisation of protective packaging systems for products and equipment. The current practice to evaluate the effectiveness of protective packaging systems dictates that prototypes are subjected to random vibration using a programmable vibration controller and shaker system. There are two approaches currently used for the laboratory simulation of the transport environment:

1) Use generic (published) Power Spectral Density (PSD) functions and test durations.

This first method involves the use of generic PSD functions which have been created by combining or averaging experimentally measured response PSD functions from various vehicle types and routes [3]. These are often published within test standards and sometimes created within individual organisations. While it is easy to obtain and use such test spectra, they fail to accurately represent the real transport environment and are often conservative which can lead to over-packaging [4].

2) Compute a test PSD function based on measured data.

This approach involves measuring vibration response data for various vehicle and route combinations, from which the PSD function(s) and root-mean-square (rms) value(s) are computed. While this approach is obviously expected to provide a more accurate representation of the transport environment than the generic spectra, significant time and resources are required to collect and analyse sufficient vibration data.

Both of these approaches make use of time compression as a way to reject low-level vibrations and shorten the test duration (for example, see [5-8]). The effectiveness and validity of time-compression as a tool to optimise protective packaging systems has been brought into question by many authors, notably [9-11]. Because of the high costs associated with the second approach, laboratory tests based on generic spectra are often chosen due to their cost-effectiveness and repeatability despite widespread doubt as to their ability to realistically simulate transport vibrations.

In the quest for an affordable alternative to generating realistic road vehicle vibration, Rouillard and Sek [12] developed an approach to synthesise realistic vehicle vibrations without the need to repeatedly collect data for each vehicle-route combination. The method requires knowledge of the road roughness properties, vehicle FRF, and the trip schedule which outlines the vehicle's speed and route information. These components are then combined to develop a test schedule to simulate the expected vibration during transport, with an outline of the method shown in Figure 1. The trip schedule in the approach uses a combination of pavement types and vehicle speeds, resulting in different target rms and PSD distributions throughout the test, and notably does not involve the use of time compression [12].

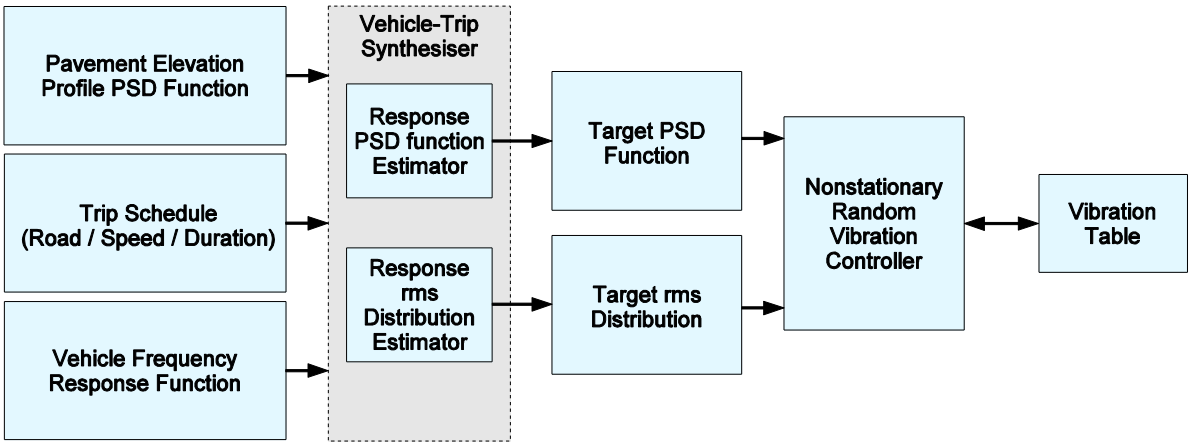

Figure 1: Outline of the technique to synthesise realistic response vibration for a particular vehicle-route combination, reproduced from [12].

As demonstrated in Figure 1, the vehicle-trip synthesis depends on three inputs. These data are generally readily available from various sources, described in further detail in this section.

1) Pavement elevation data.

Obtaining pavement roughness information is important to characterise the excitation applied to road vehicles. The PSD function of the pavement elevation profile is commonly used to describe the road roughness. The pavement elevation PSD function can be further categorised into roughness classes outlined by the International Organisation for Standardisation (ISO) under ISO standard 8608 (discussed in further detail in the following section). Pavement elevation profiles can be obtained from numerous sources. Some local authorities make the data publicly available, such as the Long-Term Pavement Performance program in the United States of America and Canada [13], or they can be obtained from local road authorities (e.g. regional departments of transport).

2) Trip schedule.

Rouillard and Sek [12] outlined two different approaches which can be implemented to develop a trip schedule. The first is a generic approach which uses reasonable ‘severity levels’ to represent vehicle speed and road roughness. The second method is more accurate and calculates the trip schedule using all the different roads’ roughness classes combined with the vehicle’s operating speed and duration travelling on each road. Once the trip schedule has been generated, the vehicle-trip synthesiser computes the target PSD function and rms level distribution which can be input directly into a vibration controller to simulate the expected vibrations of the vehicle-route combination.

3) Vehicle Frequency Response Function.

Numerous vehicle FRFs are publicly available for use, however they are all generally based on idealised quarter car models and do not represent the actual vehicle being using for transport. Some examples of readily available FRFs are presented in Figure 2. Alternatively, numerous laboratory methods are also available to experimentally establish a vehicle’s FRF. Large-scale vibration tables are commonly used and while it is relatively easy to simultaneously measure the excitation and response, these systems are expensive to acquire and maintain. Simpler experimental methods may also be employed which involve inducing a transient motion into the vehicle and measuring only the subsequent response to estimate the dynamic characteristics of the sprung mass mode. These methods are known to have limited accuracy and also require the removal of the vehicle from its normal operation. A practical method to produce

accurate estimates of the dynamic characteristics of the user's road vehicle(s) is the main limitation of the proposed vehicle vibration synthesis method. As an alternative, research into two practical approaches for accurately estimating the dynamic characteristics of road vehicles using only on-the-road vibration response data has been undertaken and the outcomes are presented in the next section.

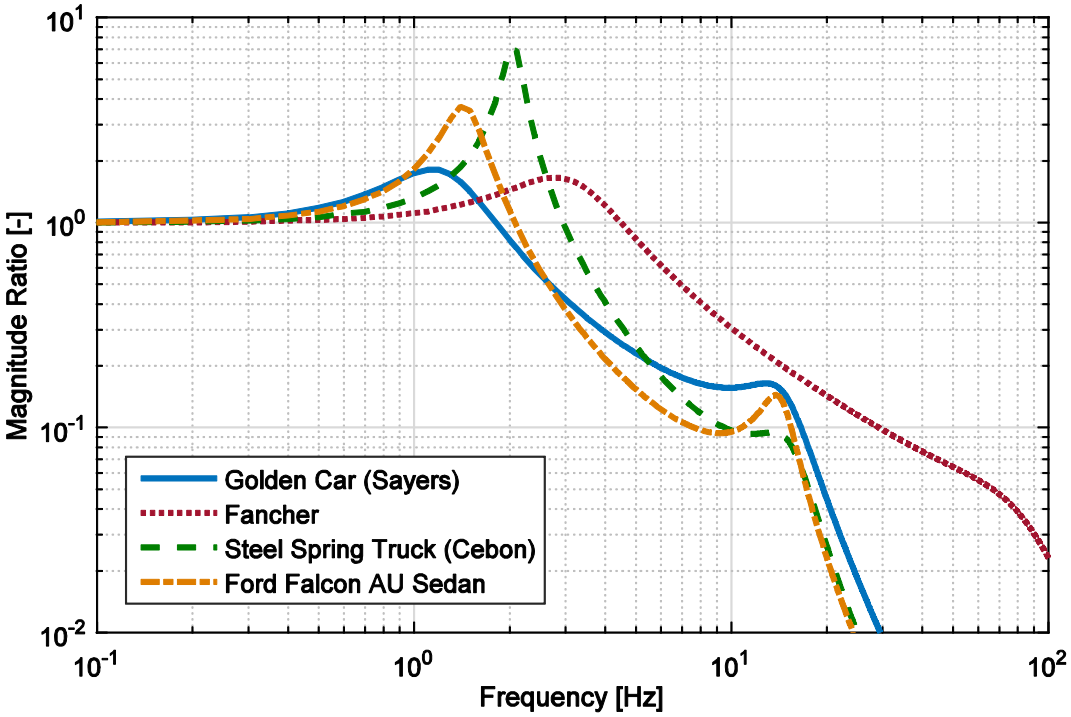

Figure 2: Typical transmissibility FRFs of some quarter car models used for simulation.

3.0 Review of Practical Approaches for Estimating the Dynamic Characteristics of Vehicles using only on-the-road Vibration Response data

In recent years, the authors have undertaken research into the development and evaluation of two different methods to estimate the FRF of road vehicles using only on-the-road vibration response data while travelling at a nominally constant operating speed. This section provides a review of these methods and the outcomes of the research. In order to provide an initial evaluation of the approaches without the complexities associated with real multi-wheeled transport vehicles, an idealised vehicle (physical quarter car) with a single wheel-spring-shock combination was commissioned and used for the on-the-road experiments. The vehicle, known as the Single-Wheeled Experimental Vehicle (SWEV), had two different configurations for the on-the-road experiments and is shown in Figure 3. The first, the SWEV-A, has the original, factory-fitted shock absorber, and the SWEV-B has a custom designed, nominally linear shock absorber. For all the on-the-road experiments, the idealised vehicle was instrumented to not only measure the sprung mass response, but also the pavement elevation profile (operates as an inertial profilometer [14]) along the wheel path to establish the actual on-the-road transmissibility FRF for validation. For a detailed description of the vehicle, see [15].

Figure 3: Photograph of the Single-Wheeled Experimental Vehicle during preliminary tests on a large-scale vibration table.

Two rural country roads (four routes) near Melbourne, Australia, were used for the on-the-road experiments: 1) route C704 with an approximate length of 40 km, denoted routes BG and GB, and 2) route C325 with a length of approximately 26 km (routes SR and RS). These routes were selected as they were deemed to be sufficiently rough for their entire length while allowing for a maximum speed of 100 km/h. Further information on the location of these routes can be found in [15].

3.1 Spectral Approach

The first approach investigated by the authors was based on the assumption that the excitation applied to the vehicle (the longitudinal pavement elevation profile(s)) could be adequately described using a predetermined spectral function. The assumed spectral function used was based on the model outlined under ISO standard 8608 [16], given in and Equation (1), and shown in Figure 4.

$$G_d(n) = G(n_0).\left(\frac{n}{n_0}\right)^{-w} [m^3] \quad (1)$$

where $G(n_0)$ is the roughness constant, n_0 is the wavenumber corresponding to 1 rad/m and the spectral exponent, w, is recommended to be 2.0.

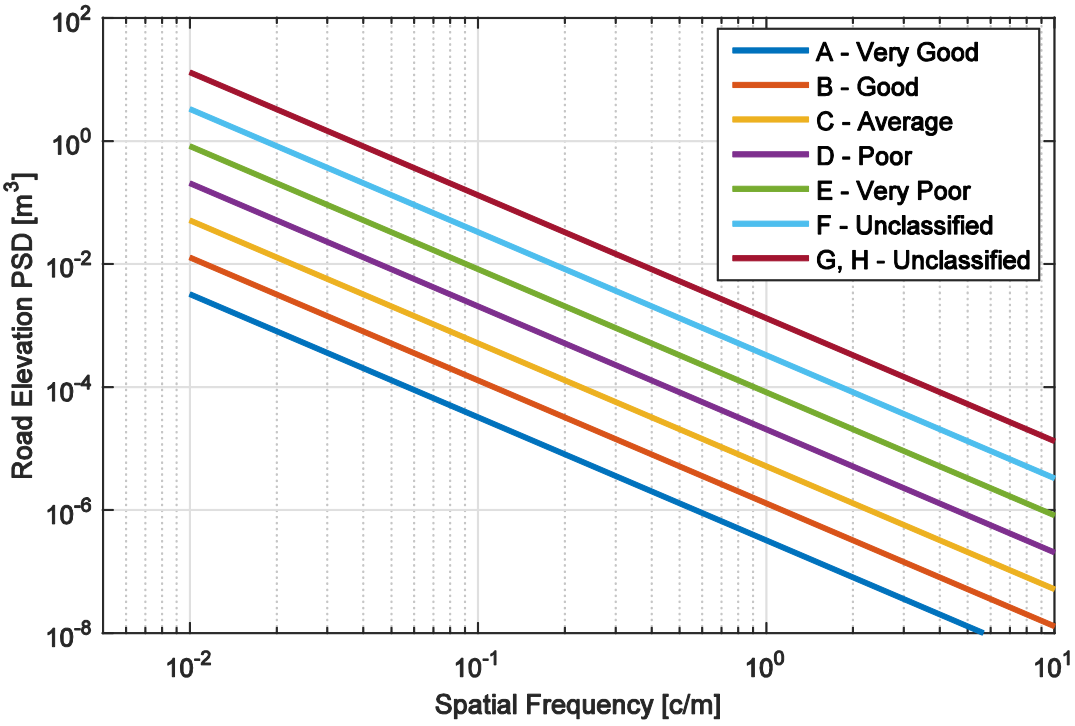

Figure 4: The ISO 8608 spectral model and road classification guide with pavement ratings from very good (A) to unclassified (F, G, H).

Several authors have found that the recommended value of the spectral exponent w = 2.0, which defines the slope of the spectral function, is rarely the case for roads which are not very long and has been found to vary between 1.5 – 3.0 [17, 18]. Provided that the pavement is long enough to allow the spectral function of the pavement to converge to the ISO model in Equation (1), then the transmissibility FRF, $T(f)$, of a quarter car vehicle travelling at a constant speed, v, can be obtained using the measured acceleration response PSD function, $R_{\ddot{x}}(f)$, and the acceleration PSD function of the ISO spectral model, $G_{\ddot{x}}(f)$, shown in Equation (2) [19].

$$T(f) = \sqrt{\frac{R_{\ddot{x}}(f)}{G_{\ddot{x}}(f)}} = \sqrt{\frac{R_{\ddot{x}}(f)}{G(f_0)}} \frac{f^{\left(\frac{w}{2}-2\right)}}{(2\pi)^2 (n_0)^{w/2}\, v^{(w/2)}} \tag{2}$$

where $G(f_0)$ is the roughness constant $G(n_0)$ converted to temporal frequency.

By driving the same vehicle over the same road at two different nominally constant operating speeds, it was conjectured that the approach could not only estimate the vehicle's FRF, but also the two parameters of the road's PSD function ($G(n_0)$ and w). The spectral exponent was estimated using the relationship derived in Equation (2) and is given in Equation (3) [19].

$$w = \frac{\ln\left(\frac{R_{\ddot{x}1}(f)}{R_{\ddot{x}2}(f)}\right)}{\ln\left(\frac{v_1}{v_2}\right)} \tag{3}$$

where $R_{\ddot{x}1}(f)$ and $R_{\ddot{x}2}(f)$ are the measured acceleration response PSD functions for two distinct nominally constant operating speeds v_1 and v_2, respectively.

The vibration response data from the on-the-road experiments were analysed to produce estimates of the vehicle FRF for a range of spectral exponent values. These were then compared with FRFs measured using a large-scale servo-hydraulic vibration table. The approach was found to not be able to accurately estimate the vehicle FRF or the spectral properties of the road. An example of the comparison between the measured transmissibility FRFs using a large-scale vibration table and on-the-road response combined with the assumed ISO 8608 spectral function is presented in Figure 5. It is clear that there is a difference between the FRFs beyond the sprung mass mode and adjusting the spectral exponent does not yield any improvement for lower magnitudes. Furthermore, considerable variation in the estimated spectral exponents using Equation (3) was observed, with a typical example presented in Figure 6.

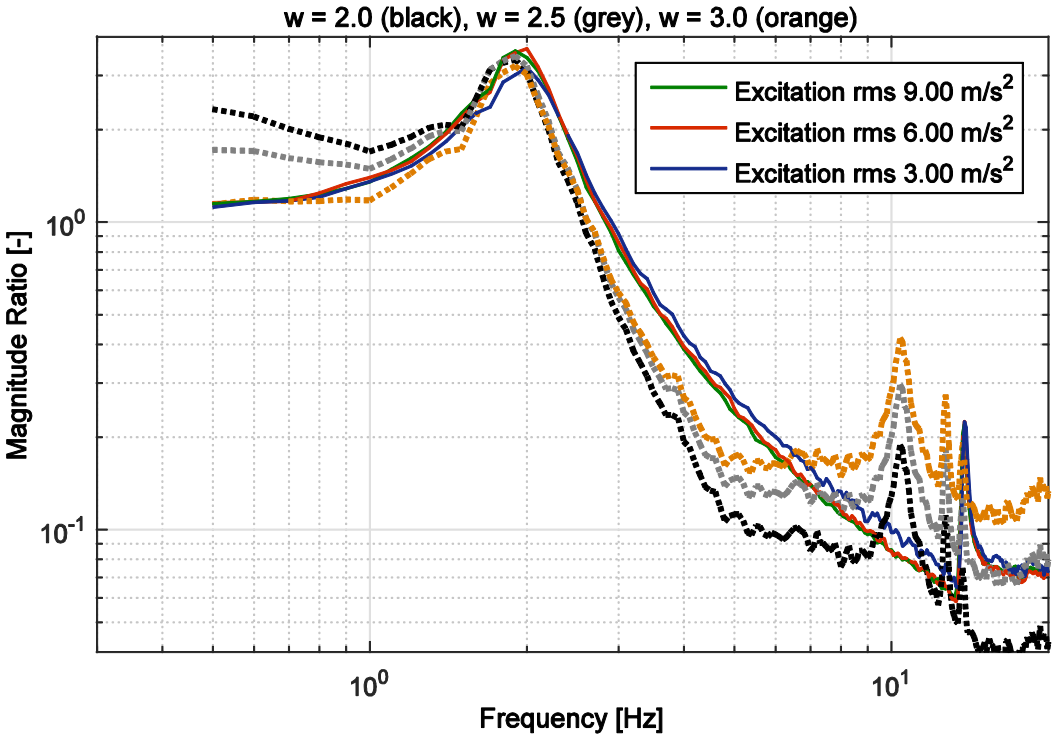

Figure 5: Comparison of the SWEV-B (100 kg) vibration table transmissibility FRFs and the estimated FRFs using on-the-road response data travelling over route BG (80 km/h) with an assumed excitation spectral exponent w set to 2.0, 2.5 and 3.0 (Δf = 0.1 Hz) [19].

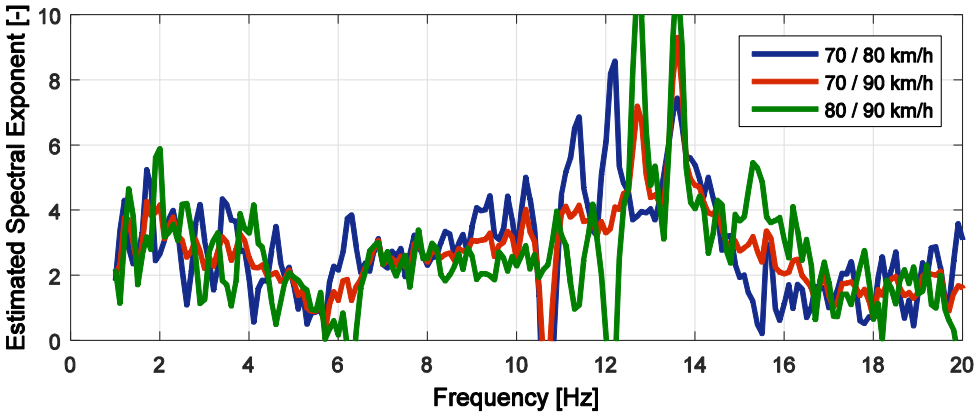

Figure 6: Typical example of the estimated spectral exponent (as a function of frequency) for various nominally constant speed ratios for the SWEV-A (50 kg) travelling over route BG, from [20].

There are numerous factors which contribute to the ineffectiveness of the approach, including:

- The spectral exponent cannot be assumed to be constant along the length of the road.
- The approach for estimating the spectral exponent is very sensitive to minor variations in the measured response spectra.
- The complex and nonlinear nature of the vehicle is too substantial for Equations (2) and (3) to hold, especially for real vehicles which can be considered as multiple-input single-output systems.

A complete description of the development and evaluation of this approach can be found in [19, 20].

3.2 Random Decrement Based Approach

A second analytical approach was developed based on the use of the random decrement technique to analyse the on-the-road vibration response data. The random decrement technique is designed to estimate the dynamic characteristics of a system using only response data and was first proposed by Henry Cole in the late 1960s to detect the failure of aerospace components [21, 22]. The initial motivation for the development of this technique was due to the difficulties encountered by Cole to measure the actual excitation during wind tunnel testing of aeronautical structural components [21]. It is important to note that common analysis techniques such as establishing the PSD function are “very dependent on the input” and so increasing the level of excitation may cause a change in the level of damping or natural frequency of the system [22].

The authors [23] developed and investigated two approaches based on the random decrement technique. The first analytical approach, known as the Hilbert approach, used the Hilbert transform to estimate the dynamic characteristics of the sprung mass mode of the vehicle. From the random decrement signatures, the Hilbert transform was used to estimate the damped natural frequency using the unwrapped instantaneous phase, and the damping ratio was estimated using the Hilbert envelope. Finally, the Single Degree of Freedom (SDoF) transmissibility FRF, in Equation (4), was then calculated. The second approach, the frequency domain approach, is based on the assumption that since the random decrement signature is proportional to the impulse response function, by taking the Fourier transform of the signature and then scaling it until it approaches unity (1) at low frequency, the vehicle’s transmissibility FRF can be estimated.

$$T(f) = \sqrt{\frac{1 + (2\zeta r)^2}{(1 - r)^2 - (2\zeta r)^2}} \tag{4}$$

where the sprung mass natural frequency is f_n, the frequency ratio is $r = f/f_n$, and ζ is the suspension damping ratio.

As part of the research, a thorough investigation into the optimum parameters for the random decrement technique was undertaken to determine the most suitable values for the random decrement signature to estimate the vehicle's FRF. Using the same on-the-road experimental vibration response, the random decrement signatures were established and analysed using the two analytical approaches. From the results, the random decrement technique in combination with the Hilbert domain approach was found to accurately estimate the FRF of the idealised vehicle, albeit limited to the sprung mass mode [23]. An example of the on-the-road measured and estimated FRFs for the two idealised vehicle configurations using the random decrement (Hilbert approach) method is shown in Figure 7. For a complete description of the development and application of the random decrement based analytical approaches, see [15, 23].

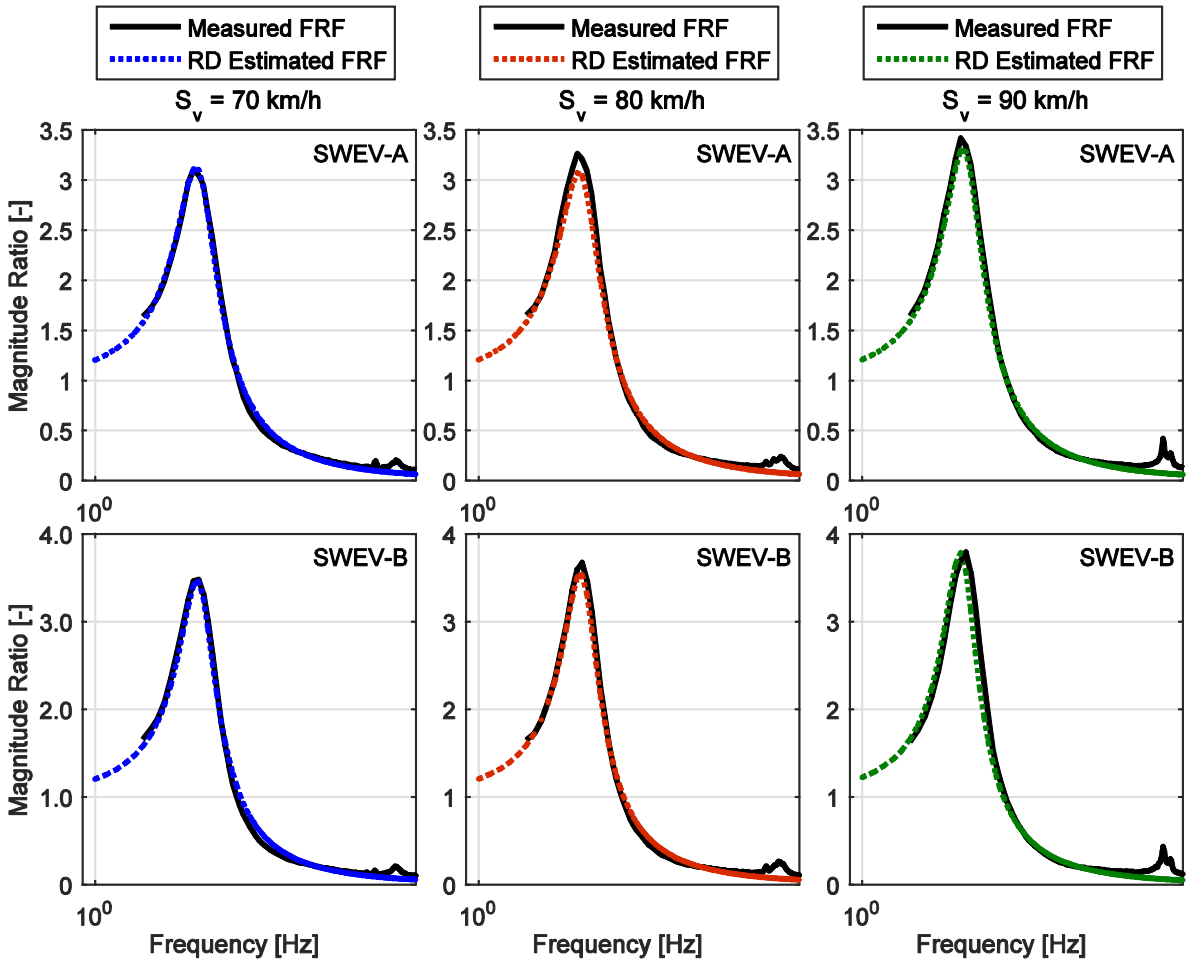

Figure 7: Comparison of the measured and estimated (random decrement – Hilbert approach) transmissibility FRFs of the SWEV-A (top row) and SWEV-B (bottom row) travelling over route BG at nominally constant operating speeds S_v of 70, 80 and 90 km/h, from [23].

4.0 Investigating the Influence of Record Length

For the on-the-road experiments, it was initially important to select a sufficiently long road to allow the pavement to converge towards the ISO 8608 [16] spectral model. It was anticipated that the length of the first selected road (routes BG and GB) would be long enough to allow for convergence to occur. The characteristics of the pavement elevation profile also play an important role and are dependent on the stationarity of the pavement under investigation. Nonstationarity of a pavement is manifested in two ways; the first is a change in the level of roughness experienced (rms) and the second is a change in the frequency structure (shape).

One important question that arises when undertaking on-the-road experiments is if there is a minimum length of road required to obtain sufficiently accurate estimates of the dynamic characteristics of road transport vehicles. Another consideration is where to begin the measurements along the selected road and if it has any significant effect on the results. The following study was undertaken using the on-the-road measured vibration records to provide an insight into the influence of: 1) the fraction of pavement from the overall length (measured vibration record), and 2) the starting point along the road. In order to address the second point, it was assumed that the road was effectively circular, i.e. the beginning and end of a route are at the same position.

4.1 Monte Carlo Simulation Procedure

A Monte Carlo simulation was employed to randomly determine the starting location of the on-the-road measurements, with a uniform statistical distribution used to provide equal opportunity for the selected starting point anywhere along the road. In order to quantify the difference for the different pavement lengths (and starting locations) the Normalised Absolute Rms Difference (NARD) is used and expressed as a percentage. A preliminary investigation into the Monte Carlo sample size found that it had a negligible impact on the estimates. The only cost incurred by increasing the estimates is the additional time required to perform the simulation, and so the selected sample size is 1,000.

The mean and standard deviation of the NARD for the 1,000 iterations for each pavement length are calculated from the time-history of the measured vibration response and the obtained random decrement signature established from the full length of the road. The data used for the Monte Carlo simulation included several sets of on-the-road vibration response data for both the SWEV-A and SWEV-B loaded with 50 kg at the sprung mass at three nominally constant operating speeds of 70, 80, and 90 km/h. Two rural roads near Melbourne, Australia, were used for the on-the-road experiments, providing four routes in total (travelling in both directions). The actual and equivalent fractions of the pavement lengths for both roads investigated using the Monte Carlo simulation are outlined in Table 1.

Table 1: Pavement length fractions and actual lengths for routes BG / GB, and SR / RS.

Pavement Length Fraction [-]	Actual Pavement Length [km]	
	Route BG / GB	Route SR / RS
1	40	26
1/2	20	13
1/4	10	6.5
1/8	5	3.25

1/16	2.5	1.625
1/32	1.25	0.8125

4.2 Rms Time-History Investigation

The results of the Monte Carlo simulation to evaluate the NARD of the on-the-road time history response are presented herein. The mean, μ, and standard deviation, σ, of the NARD of the acceleration response for various pavement length fractions are presented in Figure 8 and Figure 9 for the SWEV-A and SWEV-B travelling over route BG, respectively. A summary of the NARD is presented in Table 2 for the SWEV-A and SWEV-B travelling over routes BG and GB.

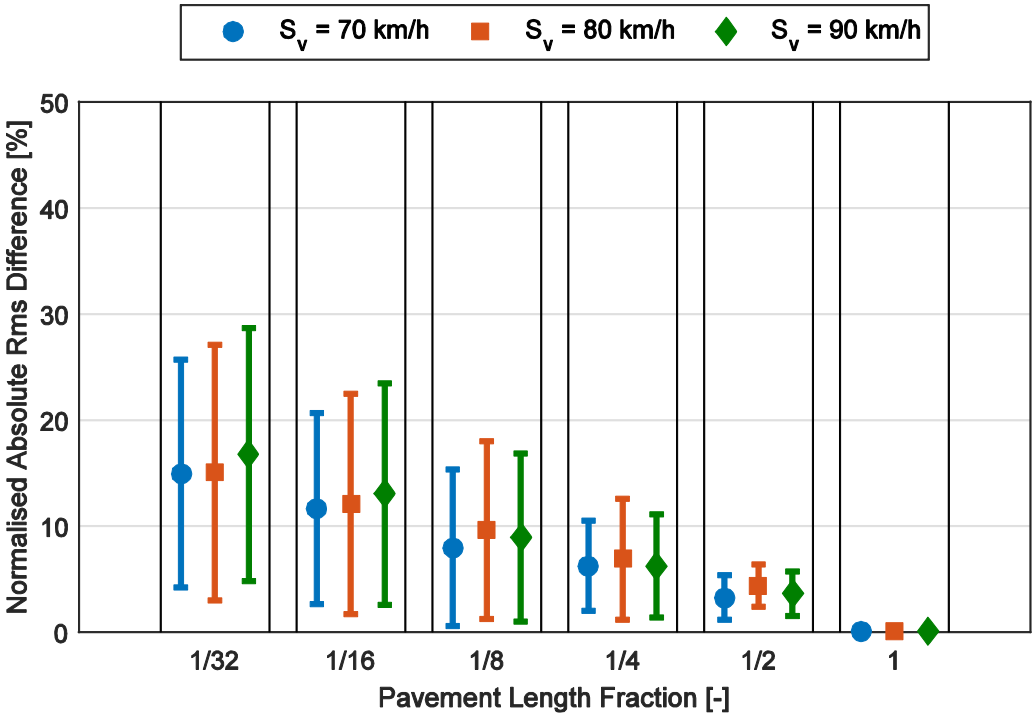

Figure 8: The mean normalised absolute rms difference (± 1σ) of the on-the-road response for various pavement length fractions using a Monte Carlo simulation (1,000 iterations) for the SWEV-A travelling over route BG.

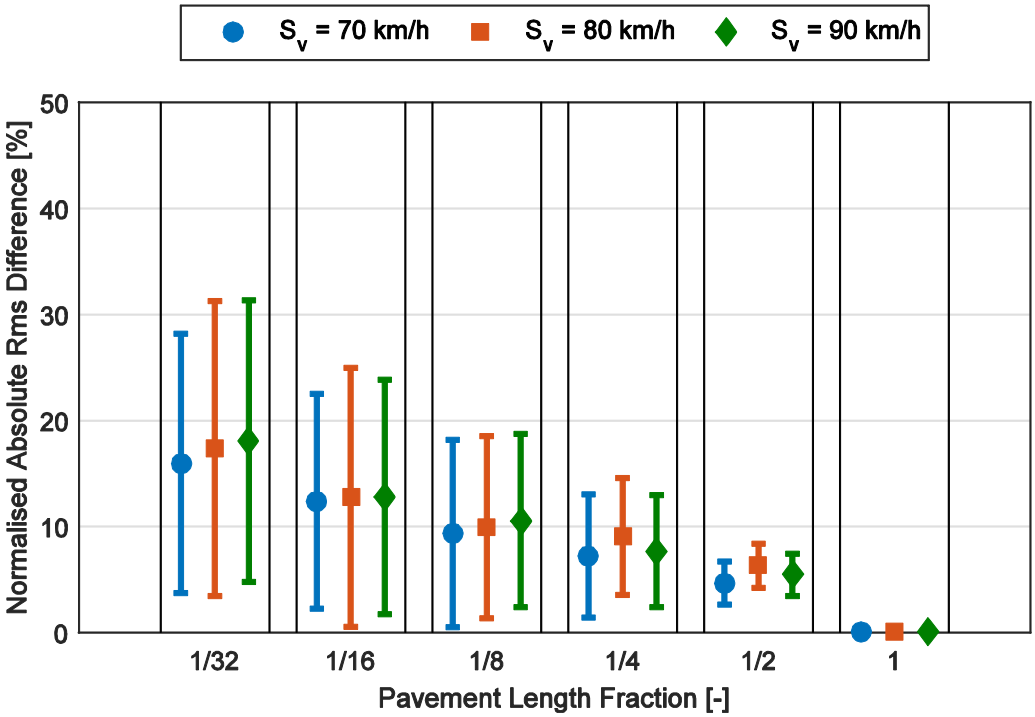

Figure 9: The mean normalised absolute rms difference (± 1σ) of the on-the-road response for various pavement length fractions using a Monte Carlo simulation (1,000 iterations) for the SWEV-B travelling over route BG.

Table 2: The mean and standard deviation of the normalised absolute rms difference of the on-the-road response for various pavement lengths using the Monte Carlo simulation (1,000 iterations) for the SWEV-A and SWEV-B travelling at various operating speeds over routes BG and GB.

Pavement Length Fraction [-]	**Normalised Absolute Rms Difference (μ ± σ) [%]**					
	SWEV-A			**SWEV-B**		
Route BG	*70 km/h*	*80 km/h*	*90 km/h*	*70 km/h*	*80 km/h*	*90 km/h*
1/2	3.3 ± 2.1	4.4 ± 2.0	3.6 ± 2.1	4.7 ± 2.0	6.3 ± 2.1	5.4 ± 2.0
1/4	6.2 ± 4.3	6.9 ± 5.7	6.2 ± 4.9	7.2 ± 5.8	9.1 ± 5.5	7.7 ± 5.3
1/8	8.0 ± 7.4	9.6 ± 8.4	8.9 ± 7.9	9.3 ± 8.8	9.9 ± 8.6	10.6 ± 8.2
1/16	11.7 ± 9.0	12.1 ± 10.4	13.0 ± 10.4	12.4 ± 10.1	12.7 ± 12.2	12.8 ± 11.1
1/32	15.0 ± 10.7	15.1 ± 12.1	16.7 ± 11.9	15.9 ± 12.2	17.4 ± 13.9	18.0 ± 13.3
Route GB	*70 km/h*	*80 km/h*	*90 km/h*	*70 km/h*	*80 km/h*	*90 km/h*
1/2	3.5 ± 1.5	3.9 ± 1.4	2.6 ± 1.5	4.6 ± 1.2	3.7 ± 1.3	3.6 ± 1.4
1/4	6.8 ± 3.1	7.4 ± 3.4	6.0 ± 3.0	7.2 ± 3.8	7.2 ± 3.4	6.8 ± 3.5
1/8	7.1 ± 5.4	7.2 ± 5.8	7.4 ± 4.9	9.00 ± 6.1	7.6 ± 5.8	8.7 ± 6.00
1/16	10.2 ± 7.0	10.1 ± 7.8	10.9 ± 7.4	11.0 ± 8.1	10.9 ± 7.9	11.2 ± 8.3

1/32	11.7 ± 8.8	13.0 ± 9.9	14.1 ± 10.7	12.8 ± 10.6	13.6 ± 10.5	15.1 ± 11.7

The Monte Carlo simulation was then repeated using the measured data obtained from routes SR and RS. Typical examples of the NARD for the SWEV-A and SWEV-B travelling over route SR are presented in Figure 10 and Figure 11, respectively. Table 3 presents the mean and standard deviation of the NARD of the time-history for the various pavement length fractions and operating speeds.

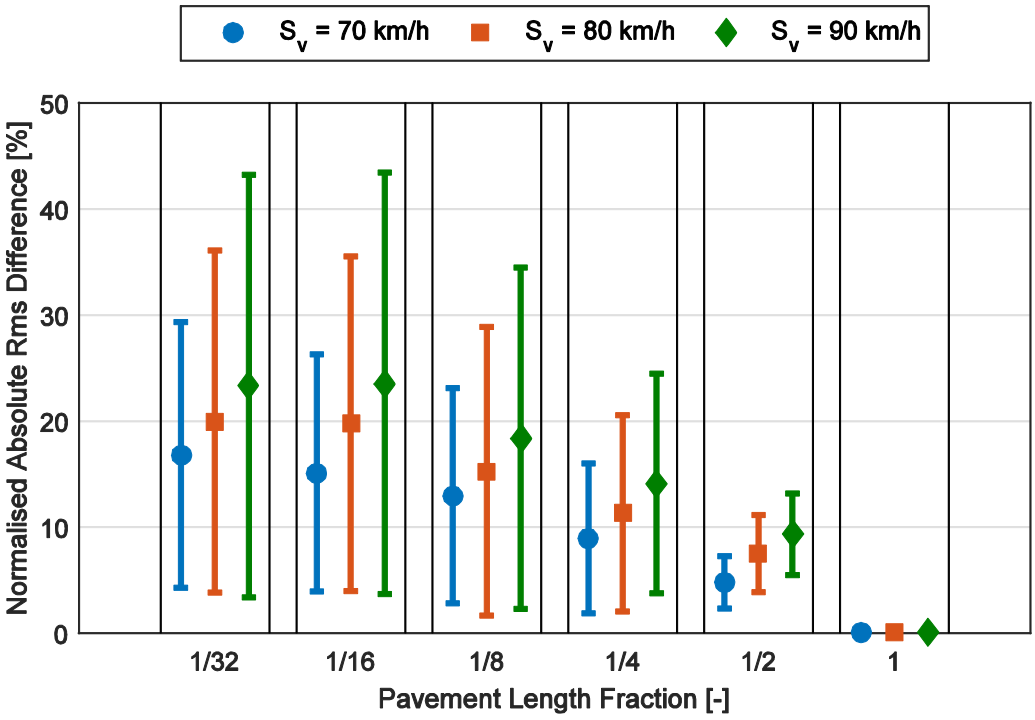

Figure 10: Typical example of the mean normalised absolute rms difference (± 1σ) of the on-the-road response for various pavement length fractions using a Monte Carlo simulation (1,000 iterations) for the SWEV-A travelling over route SR.

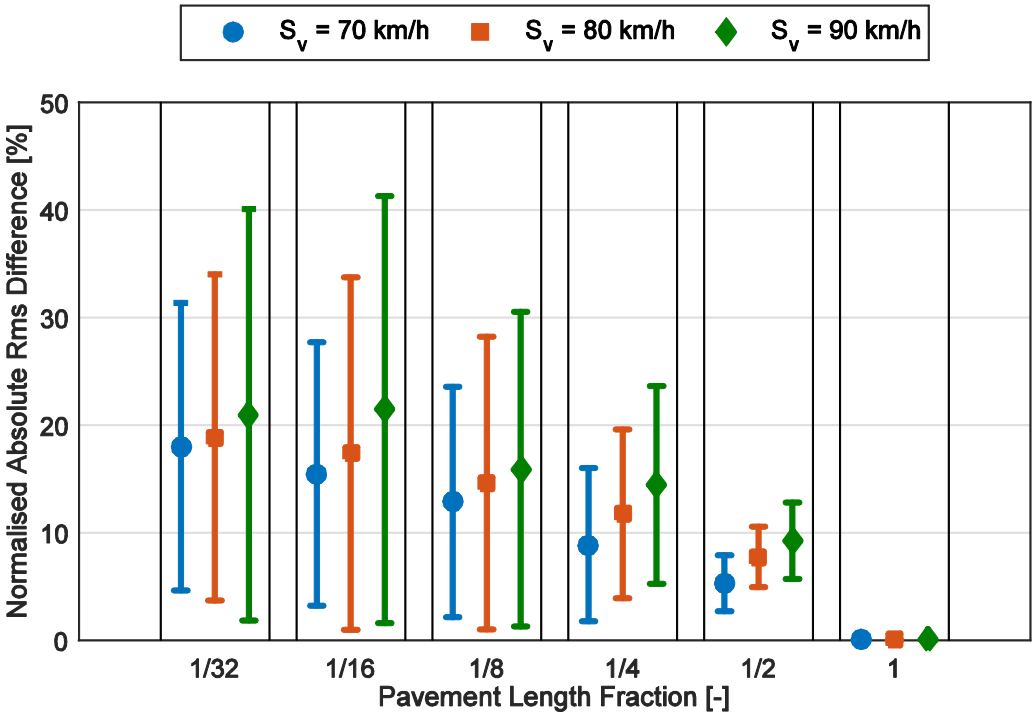

Figure 11: Typical example of the mean normalised absolute rms difference (± 1σ) of the on-the-road response for various pavement length fractions using a Monte Carlo simulation (1,000 iterations) for the SWEV-B travelling over route SR.

Table 3: The mean and standard deviation of the normalised absolute rms difference of the on-the-road response for various pavement lengths using the Monte Carlo simulation (1,000 iterations) for the SWEV-A and SWEV-B travelling at various operating speeds over routes SR and RS.

Pavement Length Fraction [-]	**Normalised Absolute Rms Difference (μ ± σ) [%]**					
	SWEV-A			**SWEV-B**		
Route SR	*70 km/h*	*80 km/h*	*90 km/h*	*70 km/h*	*80 km/h*	*90 km/h*
1/2	4.8 ± 2.5	7.5 ± 3.6	9.3 ± 3.8	5.3 ± 2.6	7.7 ± 2.8	9.2 ± 3.6
1/4	8.9 ± 7.1	11.3 ± 9.3	14.1 ± 10.4	8.9 ± 7.1	11.7 ± 7.8	14.4 ± 9.2
1/8	13.0 ± 10.1	15.3 ± 13.6	18.4 ± 16.1	12.9 ± 10.7	14.6 ± 13.6	15.9 ± 14.6
1/16	15.1 ± 11.2	19.8 ± 15.8	23.6 ± 19.9	15.4 ± 12.3	17.3 ± 16.4	21.4 ± 19.9
1/32	16.8 ± 12.5	20.0 ± 16.1	23.3 ± 19.9	18.0 ± 13.4	18.9 ± 15.2	20.9 ± 19.1
Route RS	*70 km/h*	*80 km/h*	*90 km/h*	*70 km/h*	*80 km/h*	*90 km/h*
1/2	7.3 ± 3.8	8.5 ± 4.9	9.4 ± 5.1	8.6 ± 4.2	9.1 ± 5.3	12.1 ± 4.7
1/4	10.8 ± 8.7	11.8 ± 10.6	13.4 ± 11.7	12.1 ± 10.1	12.5 ± 10.5	18.3 ± 13.3
1/8	13.3 ± 10.2	15.3 ± 11.9	16.1 ± 12.0	15.0 ± 11.5	13.9 ± 11.5	17.6 ± 15.0

1/16	14.9 ± 10.7	17.3 ± 12.8	18.8 ± 13.9	16.9 ± 12.2	16.6 ± 12.5	18.8 ± 15.4
1/32	17.2 ± 14.8	18.1 ± 13.8	21.0 ± 16.9	19.7 ± 16.2	19.2 ± 17.7	19.8 ± 18.0

For all four routes it can be seen that both the mean and standard deviation of the NARD of the rms time-history increases as the pavement length decreases. Also, as expected, the NARD is influenced by the operating speed of the vehicle, since for a given road length the duration of the measurement decreases for an increased operating speed. The considerably greater error in the equivalent pavement length fractions for routes SR and RS is due to the reduced length of the road in comparison to routes BG and GB. The results of the Monte Carlo simulation for all four routes indicate that, for any of the three nominally constant operating speeds, a sufficient estimate is obtained for a pavement length of approximately 10 km.

4.3 Rms of Random Decrement Signature Investigation

The results of the Monte Carlo simulation using the NARD of the obtained random decrement signatures are presented in this section. Typical examples of the mean and standard deviation from route BG for the SWEV-A and SWEV-B are illustrated in Figure 12 and Figure 13, respectively. Table 4 presents the mean and standard deviation of NARD of the random decrement signatures obtained for the SWEV-A and SWEV-B travelling at various operating speeds over routes BG and GB.

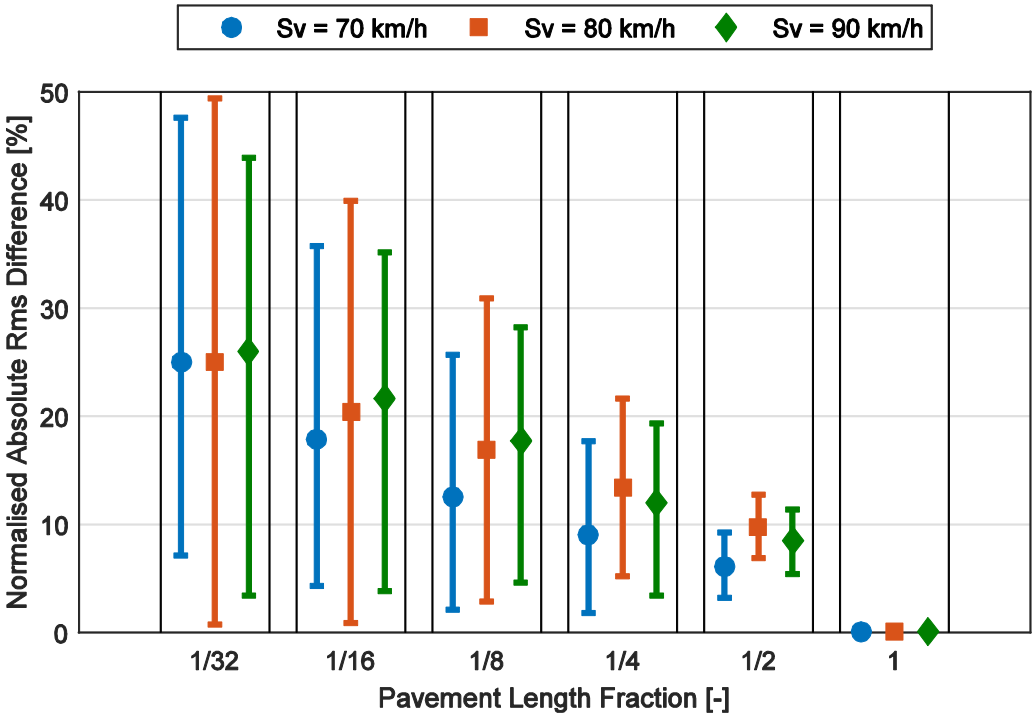

Figure 12: Typical example of the mean normalised absolute rms difference (± 1σ) of the obtained random decrement signatures for various pavement length fractions using a Monte Carlo simulation (1,000 iterations) for the SWEV-A travelling over route BG.

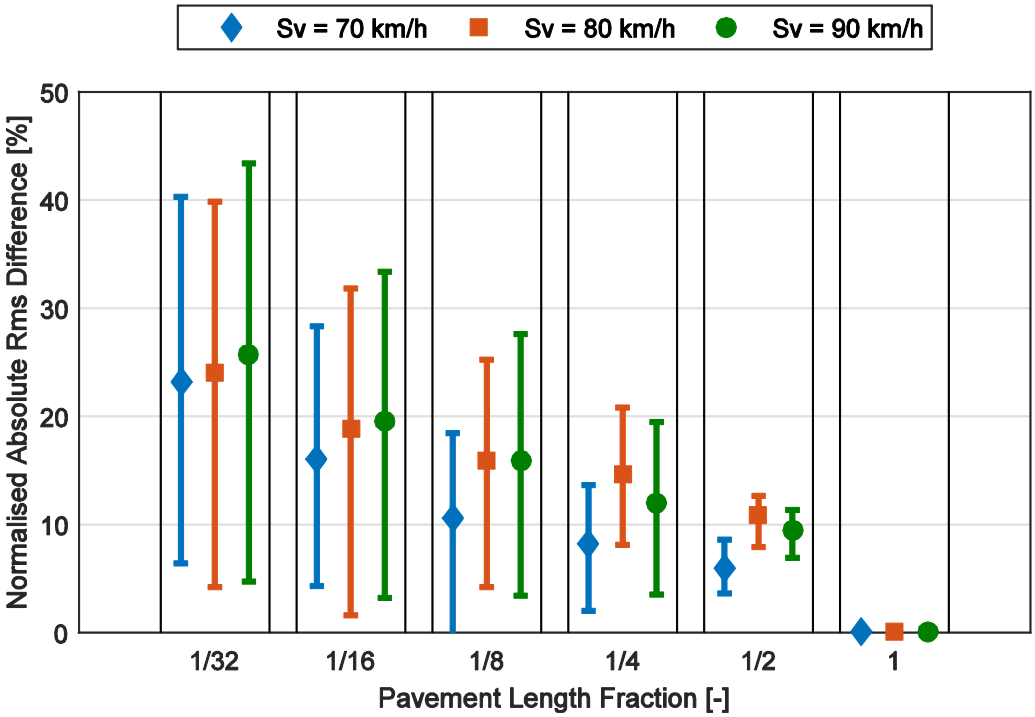

Figure 13: Typical example of the mean normalised absolute rms difference (± 1σ) of the obtained random decrement signatures for various pavement length fractions using a Monte Carlo simulation (1,000 iterations) for the SWEV-B travelling over route BG.

Table 4: The mean and standard deviation of the normalised absolute rms difference of the obtained random decrement signatures for various pavement length fractions using a Monte Carlo simulation (1,000 iterations) for the SWEV-A and SWEV-B on routes BG and GB.

Pavement Length Fraction [-]	**Normalised Absolute Rms Difference (μ ± σ) [%]**					
	SWEV-A			**SWEV-B**		
Route BG	*70 km/h*	*80 km/h*	*90 km/h*	*70 km/h*	*80 km/h*	*90 km/h*
1/2	6.1 ± 2.9	9.8 ± 2.9	8.5 ± 3.1	5.9 ± 2.3	10.9 ± 3.0	9.4 ± 2.5
1/4	9.1 ± 7.3	13.4 ± 8.2	12.0 ± 8.6	8.2 ± 6.2	14.6 ± 6.5	12.0 ± 8.5
1/8	12.6 ± 10.5	16.9 ± 14.0	17.7 ± 13.1	10.6 ± 9.7	15.9 ± 11.7	15.9 ± 12.5
1/16	17.9 ± 13.6	20.4 ± 19.5	21.6 ± 17.8	16.1 ± 11.8	18.9 ± 17.3	19.6 ± 16.4
1/32	25.0 ± 17. 9	25.1 ± 24.3	26.0 ± 22.6	23.2 ± 16.8	24.0 ± 19.8	25.7 ± 21.0
Route GB	*70 km/h*	*80 km/h*	*90 km/h*	*70 km/h*	*80 km/h*	*90 km/h*
1/2	6.6 ± 2.2	7.2 ± 2.2	5.1 ± 3.3	7.8 ± 1.9	6.9 ± 1.7	5.8 ± 2.7
1/4	11.9 ± 7.1	13.3 ± 6.6	10.6 ± 5.5	11.9 ± 7.5	11.1 ± 6.2	10.5 ± 5.4
1/8	13.7 ± 10.2	13.5 ± 11.1	13.2 ± 8.5	14.4 ± 11.7	12.1 ± 9.3	12.3 ± 7.8
1/16	18.9 ± 13.5	17.9 ± 13.3	18.5 ± 13.2	17.3 ± 13.8	18.2 ± 12.9	17.4 ± 12.2

1/32	22.1 ± 18.1	23.8 ± 19.0	24.0 ± 19.4	22.6 ± 17.7	21.9 ± 15.9	22.2 ± 17.1

The Monte Carlo simulation was repeated for routes SR and RS, with the summary of the mean and standard deviation of the NARD presented in Table 5, and typical examples are illustrated in Figure 14 for the SWEV-A and Figure 15 for the SWEV-B.

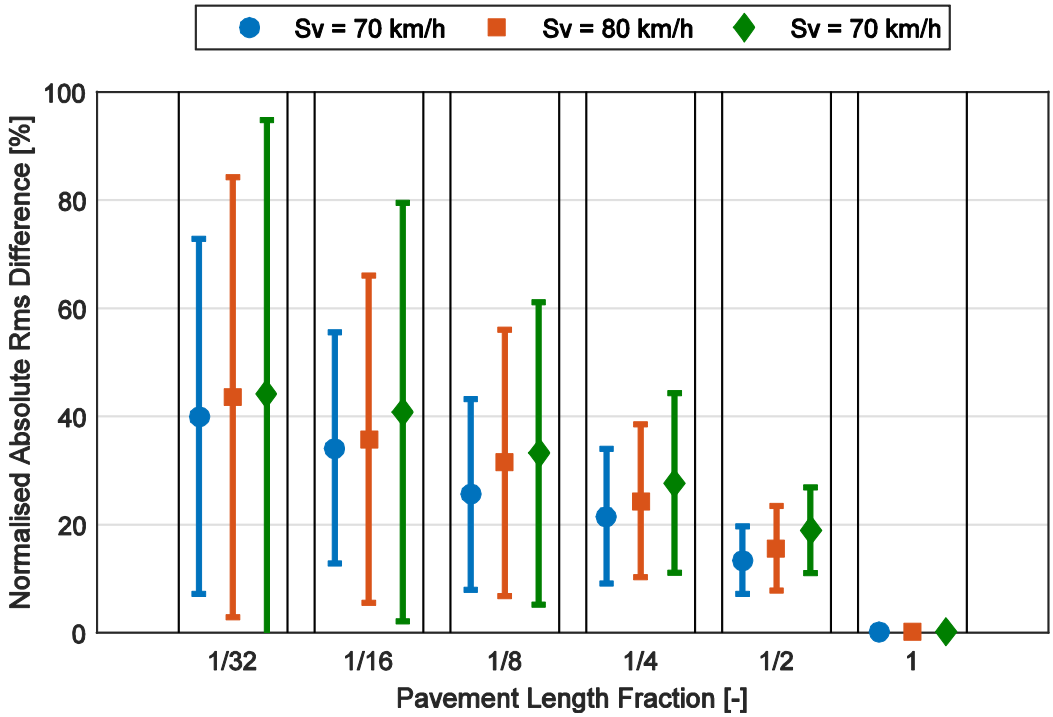

Figure 14: Typical example of the mean normalised absolute rms difference (± 1σ) of the obtained random decrement signatures for various pavement length fractions using a Monte Carlo simulation (1,000 iterations) for the SWEV-A travelling over route SR.

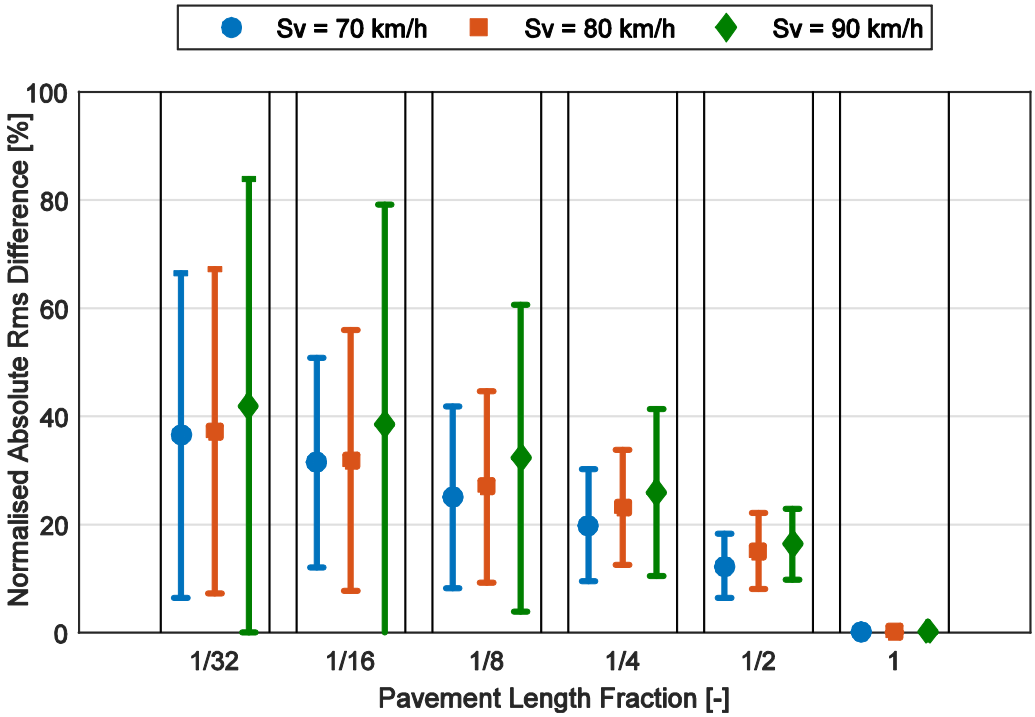

Figure 15: Typical example of the mean normalised absolute rms difference (± 1σ) of the obtained random decrement signatures for various pavement length fractions using a Monte Carlo simulation (1,000 iterations) for the SWEV-B travelling over route SR.

Table 5: The mean and standard deviation of the normalised absolute rms difference of the obtained random decrement signatures for various pavement length fractions using a Monte Carlo simulation (1,000 iterations) for the SWEV-A and SWEV-B on routes SR and RS.

Pavement Length Fraction [-]	**Normalised Absolute Rms Difference (μ ± σ) [%]**					
	SWEV-A			**SWEV-B**		
Route SR	*70 km/h*	*80 km/h*	*90 km/h*	*70 km/h*	*80 km/h*	*90 km/h*
1/2	13.4 ± 6.3	15.6 ± 7.8	18.9 ± 7.9	12.3 ± 5.9	15.1 ± 7.02	16.3 ± 6.6
1/4	21.6 ± 12.5	24.4 ± 14.2	27.7 ± 16.6	19.9 ± 10.3	23.1 ± 10.7	25.9 ± 15.4
1/8	25.5 ± 17.6	31.4 ± 24.7	33.1 ± 28.0	25.0 ± 16.8	26.9 ± 17.7	32.2 ± 28.4
1/16	34.1 ± 21.4	35.8 ± 30.3	40.8 ± 38.7	31.4 ± 19.4	31.8 ± 24.1	38.4 ± 40.7
1/32	40.0 ± 32.8	43.5 ± 40.7	44.2 ± 50.6	36.4 ± 30.0	37.2 ± 30.0	42.0 ± 41.9
Route RS	*70 km/h*	*80 km/h*	*90 km/h*	*70 km/h*	*80 km/h*	*90 km/h*
1/2	21.0 ± 10.5	22.8 ± 12.4	21.5 ± 11.5	22.0 ± 10.6	22.8 ± 11.8	20.4 ± 9.8
1/4	27.7 ± 17.1	28.8 ± 17.8	28.7 ± 19.7	28.7 ± 17.4	28.7 ± 15.9	25.3 ± 19.7

1/8	28.9 ± 18.4	30.8 ± 19.7	30.0 ± 21.4	30.0 ± 17.8	30.2 ± 17.0	29.4 ± 18.4
1/16	33.6 ± 19.7	32.1 ± 20.1	33.5 ± 23.0	34.0 ± 19.0	32.7 ± 21.0	32.0 ± 20.2
1/32	40.4 ± 32.8	36.5 ± 28.3	38.9 ± 34.8	38.2 ± 25.8	37.8 ± 30.1	36.2 ± 29.9

As noted with the rms time-history evaluation, there is a clear trend that decreasing the pavement (or record) length increases the mean and standard deviation of the NARD. However, the difference between operating speeds is not as significant for the random decrement signatures as was found for the rms time-history. It is also evident that, for the same pavement length, the NARD is much greater for the random decrement signatures than the rms time-history. In particular the mean and standard deviation of the NARD for route RS is far greater than for route SR, almost double in some cases. A pavement length of 10 – 15 km is shown to provide a suitably accurate estimate regardless of the operating speed. However, it should be noted that, when obtaining the random decrement signature, a slower nominally constant operating speed obviously provides more vibration response data and can reduce the error.

4.4 NARD and Pavement Length Fraction Results Analysis

From the results of the Monte Carlo simulation, the mean values of the NARD were then further analysed to further investigate the influence of the pavement length fraction. The obtained NARD values from both the rms time-history and rms of the random decrement signatures were separated by the two roads. The influence of the vehicle was also examined by separating the SWEV-A and SWEV-B results, but no clear distinction between the obtained NARD values was observed. The results of the analysis are shown in Figure 16, and the NARD was found to follow a general power law relationship shown in Equation (5). The results of the curve-fit, including the coefficients of determination, are given in Table 6. While there is noticeable scatter in the results (particularly for the routes SR and RS), it is evident that as the pavement length ratio is increased the NARD decreases. It should be noted that this is only a small-scale investigation and further routes are required to statistically show that this relationship holds for other road and vehicle combinations.

$$NARD = aP^{-b} \tag{5}$$

where P is the pavement length fraction, and a and b are both constants.

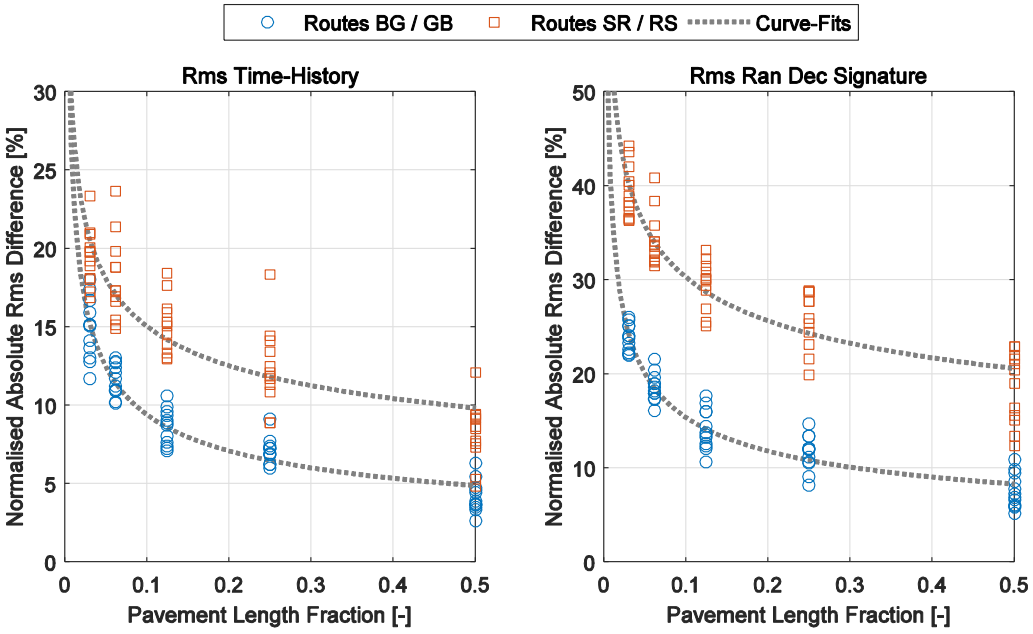

Figure 16: The best-fitting curves of the NARD vs. pavement length fraction obtained from the Monte Carlo simulation for the rms time-history (left) and the rms of the random decrement signatures (right).

Table 6: The parameter values for the curve-fits and the coefficients of determination from the NARD and pavement length fraction investigation.

	Rms Time-History			Rms Random Decrement Signature		
	a	*b*	R^2	*a*	*b*	R^2
Routes BG / GB	3.68	0.41	0.89	6.36	0.38	0.91
Routes SR / RS	8.19	0.26	0.73	17.42	0.24	0.83

5.0 Experimental Procedure for Vehicle FRF Estimation

Having validated the random decrement (Hilbert approach) based method, a guide on best practices for the on-the-road measurements was developed. This section describes the experimental procedure to undertake on-the-road vehicle vibration measurements and provides guidelines for best measurement practices to estimate the vehicle's FRF (limited to the sprung mass mode).

5.1 Considerations for undertaking on-the-road vehicle vibration measurements

One of the most important factors to consider when undertaking on-the-road experiments is to ensure that any changes in vehicle speed are avoided or minimised. In particular, the selected road section should not have traffic lights, intersections which require stopping, steep ascents or descents, sharp corners, and high traffic roads (particularly during peak hours). Under normal conditions, a vehicle's operating speed will vary significantly and it is practically impossible to avoid these factors. The recommended approach for dealing with any vehicle speed variation is to simultaneously measure the vehicle speed (preferably synchronised with the vibration measurements) and, during post processing, exclude those segments of data which are outside the permissible range (as done in the real vehicle case study in the following section). The recommended parameters for the measurement and pre-processing of the on-the-road response data from transport vehicles to estimate the dynamic characteristics is presented in Table 7. It is

worthwhile to reiterate that if a general on-the-road measurement is made, then a higher sampling frequency will be required to record the effects of higher modes.

Table 7: The recommended parameters and conditions for the on-the-road measurement and pre-processing of vehicle vibrations.

Parameter	**Value**
Sampling Frequency	200 Hz
Low-Pass Filter:	
- Order	5
- Cut-Off Frequency	8 Hz
Exclude vibration events outside target speed	± 3 km/h
Minimum recommended pavement length	10 – 15 km

Another important factor is the location of the vibration recording device on the transport vehicle. Care must be exercised by the user when selecting the location to mount the vibration sensor to ensure that the correct dynamic motion is measured. The location of the sensor should also avoid coordinate coupling, which can introduce additional tangential acceleration components due to the pitch and roll of the vehicle during operation. While few references exist in regards to the consideration and selection of the measurement location for vehicles, an example of the effects of measurement location on heavy vehicle ride is given by Gillespie [24].

5.2 Analysis of on-the-road vibration response data

Once the on-the-road experimental measurements have been completed, the vibration response is processed using the recently developed random decrement based approach to estimate the dynamic characteristics (FRF) of the vehicle [23]. A flow chart of the analysis procedure for the response data is presented in Figure 17. First, the measured response data is pre-processed before the random decrement signature is established. If the speed has been monitored throughout the on-the-road experiments (as recommended), then any events which fall outside the desired nominally constant operating speed range (± 3 km/h) must be excluded. A low-pass filter is applied to the response data in order to isolate the sprung mass mode.

The optimum parameters for establishing the random decrement signature from vehicle vibration response data are given in Table 8. From the random decrement signature, the Hilbert transform is used to establish the instantaneous phase and the Hilbert envelope in order to estimate the sprung mass damped natural frequency and damping ratio, respectively. These estimates are then input into the SDoF transmissibility FRF model from Equation (4). This procedure can be repeated for the remaining on-the-road measurements (e.g. for different operating speeds if desired). A detailed description of the analysis procedure is described in [15, 23].

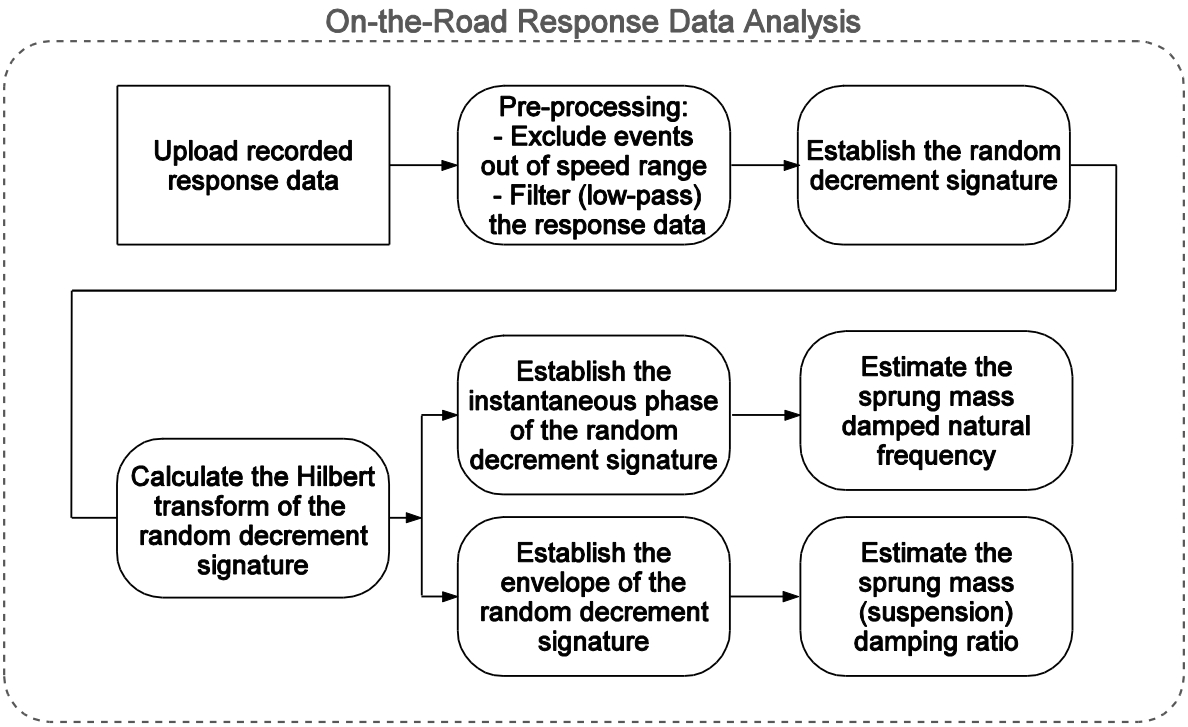

Figure 17: Flow chart of the general procedure for analysing the measured on-the-road response data.

Table 8: The optimum parameters to establish the random decrement signature, from [23].

Random Decrement Parameter	Value / Condition
Trigger Type	Trigger Up
Trigger Level	Zero-Crossing
Trigger Spacing	None
Minimum Number of Averages, N_{RD}	500

6.0 Discussion and Conclusions

This paper describes a practical approach for the accurate estimation of vehicle dynamic characteristics, namely the vehicle FRF, using only on-the-road response data. A review of two approaches for estimating the dynamic characteristics using only on-the-road response data developed by the authors was presented. The techniques were evaluated using an idealised, physical quarter car vehicle, and the results found that the approach using the random decrement method in combination with the Hilbert transform obtained the most accurate estimates of the dynamic characteristics of the sprung mass mode of the idealised vehicle.

With the random decrement based approach established using the idealised vehicle, an investigation was then undertaken into the length of pavement (i.e. record length) required to obtain a sufficient estimate of the response spectrum and random decrement signature. The investigation was undertaken using a Monte Carlo simulation (1,000 iterations) to randomly select a starting point along the road for a variety of selected pavement length fractions. The mean and standard deviation of the NARD from each of the samples with a random starting location was established and compared with the estimates obtained from the full length of the routes.

The measured responses of the SWEV-A and SWEV-B (sprung mass loaded with 50 kg) configurations over two roads (four routes) were evaluated using a Monte Carlo simulation for three nominally constant operating speeds. While the results are only indicative, the simulation suggests that a minimum road length of 10 km is generally sufficient to establish reasonable estimates of the dynamic characteristics, or FRF, of a road vehicle. The random decrement signature, in some cases (particularly for the shorter road SR / RS investigated) provides sufficient estimates for a minimum pavement length of 10 – 15 km.

A comprehensive guide to undertaking on-the-road vehicle vibration measurements and analysis of the response data is also included. This includes a practical guide on setting up and undertaking the on-the-road experiments, along with an outline of the general analysis procedure using the random decrement and Hilbert transform analysis technique. Having established the technique and provided an initial investigation into the minimum record length required, future work to be undertaken will focus on a series of case studies involving real transport vehicles. Other avenues identified for further research are the development of an improved FRF model that is able to include the unsprung mass mode, and to investigate the influence of speed variation on the dynamic characteristics.

References

1. Ostergaard, S., *Packaging goals in transport quality*, in *7th IAPRI World Conference on Packaging*. 1991: Utrecht, Holland.
2. Sek, M. *Optimisation of Packaging Design Through an Integrated Approach to the Measurement and Laboratory Simulation of Transportation Hazards*. in *12th International Conference on Packaging*. 2001. Warsaw, Poland.
3. Materials, A.S.o.T.a., *Standard Practice for Performance Testing of Shipping Containers and Systems: D4169-08*. 2009: West Conshohocken.
4. Rouillard, V., *Generating road vibration test schedules from pavement profiles for packaging optimization.* Packaging technology and Science, 2008. **21**(8): p. 501-514.
5. *Test Method Standard MIL-STD-810G*. 2008, United States Department of Defence: Maryland.
6. *Standard 00–35 Environmental Handbook for Defence Materiel Part 5 Issue 4 Induced Mechanical Environments*. 2006, United Kingdom Minisitry of Defence: Glasgow, UK.
7. *Standard Test Method for Random Vibration Testing of Shipping Containers D4728-06*. 2012, ASTM International.
8. Fleetwood, K.G., *Near-field blast vibration monitoring and analysis for prediction of blast damage in sublevel open stoping*, in *Department of Mining Engineering and Surveying*. 2010, Curtin University: Perth, Australia.
9. Charles, D., *Derivation of environment descriptions and test severities from measured road transportation data.* Journal of the Institute of Environmental Sciences, 1993. **36**(1): p. 37-42.
10. Rouillard, V. and M. Sek, *Monitoring and simulating non-stationary vibrations for package optimization.* Packaging Technology and Science, 2000. **13**(4): p. 149-156.
11. Shires, D., *On the time compression (test acceleration) of broadband random vibration tests.* Packaging Technology and Science, 2011. **24**(2): p. 75-87.
12. Rouillard, V. and M. Sek, *Creating transport vibration simulation profiles from vehicle and road characteristics.* Packaging Technology and Science, 2013. **26**(2): p. 82-95.
13. *LTPP InfoPave*. 2016; Available from: https://infopave.fhwa.dot.gov/.
14. Spangler, E.B. and W.J. Kelly, *GMR road profilometer-a method for measuring road profile.* Highway Research Record, 1966(121).
15. Ainalis, D., *Estimating the Dynamic Characteristics of Road Vehicles Using Vibration Response Data*, in *College of Engineering and Science*. 2014, Victoria University: Melbourne, Australia.
16. Standardisation, I.O.f., *International Standard 8608: Mechanical Vibration - Road Surface Profiles - Reporting of Measured Data*. 1995: Geneva.
17. Andren, P., *Power spectral density approximations of longitudinal road profiles.* International Journal of Vehicle Design, 2005. **40**(1-3): p. 2-14.

18. Kropac, O. and P. Mucka, *Indicators of longitudinal unevenness of roads in the USA.* International journal of vehicle design, 2008. **46**(4): p. 393-415.
19. Ainalis, D., V. Rouillard, and M. Sek, *Issues with combining road elevation spectral models and vehicle vibration response to estimate vehicle dynamic characteristics.* Packaging Technology and Science, 2015. **28**(3): p. 253-270.
20. Ainalis, D., V. Rouillard, and M. Sek, *On-the-road Measurements to Establish the Dynamic Characteristics of Transport Vehicles.* Packaging Technology and Science, 2015.
21. Cole Jr, H.A., *On-line analysis of random vibrations.* Journal of the American Institute of Aeronautics and Astronautics, 1968.
22. Cole, H.A., *On-line failure detection and damping measurement of aerospace structures by random decrement signatures*. Vol. 2205. 1973: National Aeronautics and Space Administration.
23. Ainalis, D., V. Rouillard, and M. Sek, *Estimating the ride quality characteristics of vehicles with random decrement analysis of on-the-road vibration response data.* Vehicle System Dynamics, 2016. **54**(6): p. 765-783.
24. Gillespie, T.D., *Heavy truck ride*. 1985, SAE Technical Paper.